Geophysical Research Letters

RESEARCH LETTER
10.1002/2017GL076320

Seasonal Outflow of Ice Shelf Water Across the Front of the Filchner Ice Shelf, Weddell Sea, Antarctica

E. Darelius[1] **and J. B. Sallée**[2]

[1]Geophysical Institute, University of Bergen and the Bjerknes Centre for Climate Research, Bergen, Norway, [2]Sorbonne Universités, CNRS, LOCEAN, Paris, France

Key Points:
- A 4-year long mooring record shows seasonal outflow of ISW across the western part of the Filchner ice shelf front
- We hypothesize that the outflow is linked to observed changes in the stratification through PV dynamics
- The outflow of ISW across the eastern part of the ice shelf front is more persistent

Supporting Information:
- Supporting Information S1

Correspondence to:
E. Darelius,
elin.darelius@uib.no

Citation:
Darelius, E., & Sallée, J. B. (2018). Seasonal outflow of ice shelf water across the front of the Filchner ice shelf, Weddell Sea, Antarctica. *Geophysical Research Letters*, *45*. https://doi.org/10.1002/2017GL076320

Received 20 NOV 2017
Accepted 25 MAR 2018
Accepted article online 19 APR 2018

Abstract The ice shelf water (ISW) found in the Filchner Trough, located in the southern Weddell Sea, Antarctica, is climatically important; it descends into the deep Weddell Sea contributing to bottom water formation, and it blocks warm off-shelf waters from accessing the Filchner ice shelf cavity. Yet the circulation of ISW within the Filchner Trough and the processes determining its exchange across the ice shelf front are to a large degree unknown. Here mooring records from the ice shelf front are presented, the longest of which is 4 years long. They show that the coldest ($\Theta = -2.3°C$) ISW, which originates from the Ronne Trough in the west, exits the cavity across the western part of the ice shelf front during late austral summer and early autumn. The supercooled ISW escaping the cavity flows northward with a velocity of about 0.03 m/s. During the rest of the year, there is no outflow at the western site: the current is directed eastward, parallel to the ice shelf front, and the temperatures at the mooring site are slightly higher ($\Theta = -2.0°C$). The eastern records show a more persistent outflow of ISW.

Plain Language Summary Antarctica is surrounded by large, floating ice shelves covering vast ice shelf cavities that are filled with sea water. The circulation of water within the cavity brings heat toward the ice shelf base, which causes the ice shelves to melt from below. To understand the future evolution of the Antarctic ice shelves and the ice sheet upstream, we need to understand the physics governing the sub-ice shelf circulation and the processes determining the heat transport across the ice shelf front. Here we present mooring records from the front of the Filchner ice shelf in the Weddell Sea, Antarctica. The unique records show that there is a seasonal outflow of water that has been cooled down below the surface freezing point temperature through interaction with the glacial ice, across the western part of the front. The outflow across the eastern part of the front is stronger, more persistent, and slightly warmer. It is hypothesized that the seasonality in the western outflow is caused by changes in the stratification. The findings reopens the question about the potential blocking effect caused by the large step in bathymetry effectuated by the ice shelf front.

1. Introduction

The interaction between the floating ice shelves fringing the Antarctic continent and the ocean water filling their cavities is central to the mass balance of the Antarctic ice sheet (Fürst et al., 2016; Pritchard et al., 2012). At the same time, water masses formed within the cavities are in some locations known to descend the continental slope and contribute to the formation of Antarctic bottom waters, a principal component in the global thermohaline circulation (e.g., Foldvik et al., 2004). In other locations, the fresh water input from ice shelf melt inhibits bottom water formation (Hellmer, 2004). The rate at which water enters and exits the ice shelf cavities and the degree to which it interacts with the meteoric ice will hence influence both the stability of the Antarctic ice sheet and the properties of the abyssal ocean.

The Filchner-Ronne ice shelf (FRIS), located in the southwestern Weddell Sea, is the largest (by volume) ice shelf in Antarctica. The majority of the water entering the FRIS cavity is at the surface freezing temperature (Nicholls et al., 2009), and basal melt rates are currently low (Rignot et al., 2013). The export of ice shelf water (ISW) emerging from the FRIS (see Figure 1 for locations) through the Filchner Trough (FT) forms the Filchner overflow (Darelius et al., 2009; Foldvik et al., 2004) and contributes to the formation of Antarctic bottom waters. Recent modeling efforts suggest that the presence of relatively dense ISW in the FT prevents it from being flooded by warmer off-shelf water masses, thus limiting the basal melt rates below FRIS (Hellmer et al., 2012, 2017).

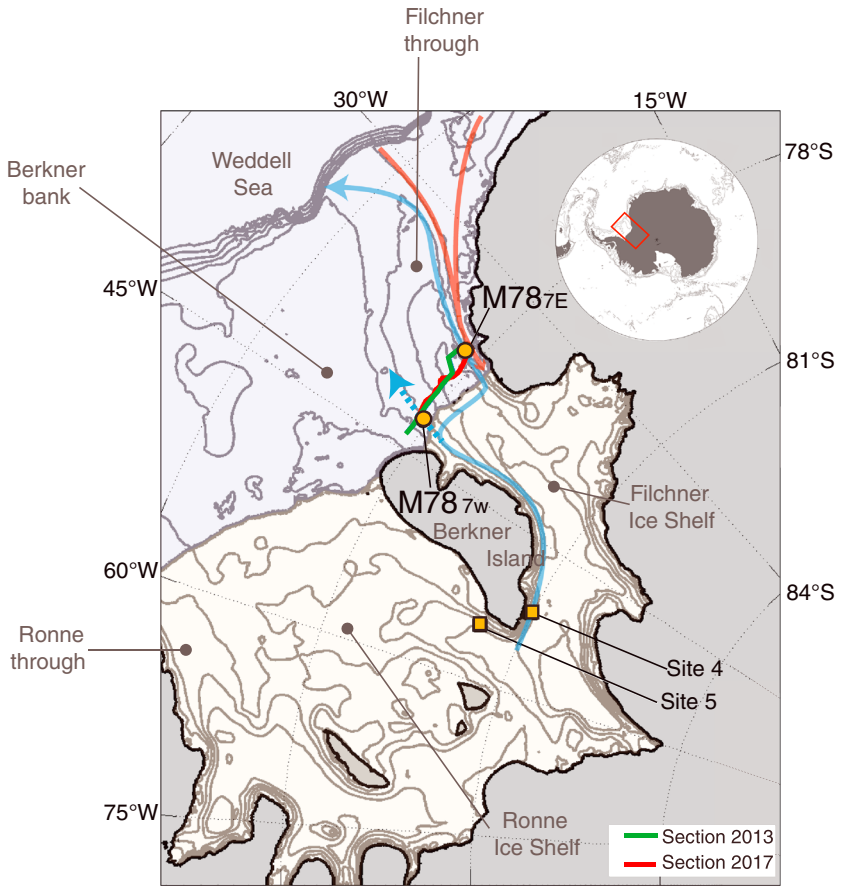

Figure 1. Map showing the bathymetry of the study region and the circulation in the region as suggested by Darelius, Makinson, et al. (2014) and Nicholls et al. (2009). The red arrows show the seasonal inflow of water across the continental shelf break, while the blue arrows show the path of the ice shelf water. The position of the conductivity-temperature-depth sections and the moorings are indicated according to the legend. Grounded ice is shown in gray, ice shelves in white, and ocean in light blue. The inset shows the location of the study area (red rectangle). Bathymetry contours are shown every 200 m.

The ISW filling the FT (Carmack & Foster, 1975) is formed as high salinity shelf water (HSSW) produced on the wide continental shelf in the west, enters the ice shelf cavity, and interacts with the glacial ice (Nicholls et al., 2009). Within the cavity, the HSSW is cooled and slightly freshened as it melts the ice above it on its way around the southern tip of the Berkner Island and northward toward the front of the Filchner ice shelf (FIS) (Nicholls et al., 2001, 2009, see Figure 1). Numerical modeling suggests that the sudden shift in water column thickness at the ice shelf front forces the ISW to follow the FIS front eastward before exiting the cavity (Darelius, Makinson, et al., 2014). The ISW, which is potentially supercooled (i.e., at a temperature lower than the surface freezing point), then flows northward along the eastern flank of the FT (Darelius, Makinson, et al., 2014; Ryan et al., 2017) toward the sill where it overflows at a rate of 1.6±0.5 Sv (Foldvik et al., 2004). The severe sea ice conditions make the FT region inaccessible during winter, and observations have been limited to the short summer season (with exception of sparse conductivity-temperature-depth [CTD] profiles collected by Weddell Seals; Årthun et al., 2013). Hydrographic profiles obtained during ice-free summers in the region just north of the FIS front show variability in the properties of ISW that points to variability of their source water, that is, variability in the properties of HSSW entering the cavity (Darelius, Makinson, et al., 2014, their Figure 3c). HSSW with an absolute salinity (S_A) higher than about 34.92 is typically associated with HSSW originating from the Ronne Trough (west of 55°W), while HSSW of lower salinity ($S_A \simeq 34.84$) is thought to originate from the Berkner Bank. Hereafter, we refer loosely to ISW with a source salinity higher than 34.92 as ISW_{Ronne}, and ISW with a source salinity around 34.84 as $ISW_{Berkner}$, although it is uncertain to what extent the properties of the HSSW remain constant in time. While ISW_{Ronne} was reported at the FIS front in summer 1977, 1993, 1995, 2011,

and 2017, the water mass was not observed there in 1980, 1984, and 2013 (Darelius, Makinson, et al., 2014 their Figure 3, and Figure 4a, this paper). The observed variability in ISW properties was suggested by Darelius, Makinson, et al. (2014) to be interannual, but here we demonstrate that the variability is partly explained by seasonal variability in the outflow of ISW across the FIS front. While sub-ice shelf observations and modeling show that there is a pronounced seasonality in the flow of HSSW into the cavity across the front of the Ronne ice shelf, the lack of winter time observations from the FIS front has prevented us from determining if there is a seasonality also in the outflow. The inflow of HSSW peaks during midwinter when the HSSW production is most intense and shows a smaller, secondary peak during summer (Jenkins et al., 2004). The seasonality is, however, much reduced in the Filchner part of the cavity (Jenkins et al., 2004; Nicholls & Østerhus, 2004). In the northern part of the FT, the flow of ISW across the sill shows a seasonality in water mass properties but not in outflow velocity (Darelius, Strand et al., 2014). Observations from the continental shelf east of the FT show a pronounced seasonality in the circulation. The summer time inflow of modified warm deep water (Årthun et al., 2012; Darelius et al., 2016) stops in winter when the thermocline depth above the continental slope increases (Semper & Darelius, 2017) and the water column above the continental slope is homogenized by convection (Ryan et al., 2017).

This paper describes the outflow of ISW across the FIS front based on records from two oceanic moorings deployed in the vicinity of the ice shelf front in 2013. The mooring records are up to 4 years long and provide the first time series of oceanic conditions from the FIS front.

2. Data

Two oceanic moorings equipped with temperature, conductivity (not used here), and pressure sensors as well as current meters were deployed just north of the FIS front in January 2013. $M78_{7W}$ (77.92°S, 42.16°W) was deployed at 700-m depth on the western side of the FT, about 3 km from the ice shelf front, and $M78_{7E}$ (77.75°S, 36.15°W, called M_{south} in Darelius et al., 2016) was deployed along the 700-m isobath on the eastern side of the FT (Figure 1). Due to thick fast ice in front of the ice shelf, $M78_{7E}$ was deployed about 20-km north of the front. $M78_{7E}$ was recovered in February 2014 and $M78_{7W}$ in February 2017, then only being 400 m from the advancing FIS front.

Frazil ice may form at depth within in situ supercooled ISW (Fer et al., 2012; Foldvik & Kvinge, 1974). An accumulation of frazil ice on the instrument originally placed at 480-m depth at $M78_{7W}$ caused it to slide up the mooring line in May 2014. The ascending instrument brought two instruments clamped onto the line with it to the top of the mooring (380-m depth), where they remained until mooring recovery. Pressure records from the top of the moorings show that the pull-down due to current drag was smaller than 5 m 99% of the time, and the related changes in instrument depths have been ignored.

The current meter records—obtained from an RDI 150 kHz acoustic Doppler current profiler in the east and Aanderaa point current meters in the west—were corrected for magnetic declination using the deployment mean value (9.3°E and 5.1°E for $M78_{7W}$ and $M78_{7E}$, respectively) obtained from www.ngdc.noaa.gov/geomag-web/#declination. CTD sections along the front were obtained during mooring deployment and recovery (Figure 2). Salinities are reported in absolute salinity, S_A (IOC et al., 2010), with δS_A taken from version 3.6 of McDougall et al. (2012) database. Note that the S_A values in this region are about 0.17 higher than values obtained when using practical salinities. Similarly, temperatures are reported in conservative temperature, Θ (IOC et al., 2010).

The ice shelf draft shown in the figures is obtained from Bedmap2 (Fretwell et al., 2013) at 78.3°S.

3. ISW Outflow

The temperature records from $M78_{7W}$ show a distinct seasonal cycle with a reoccurring pulse of cold ISW ($\Theta < -2.25$°C) appearing at the mooring site between February and May–June each year (Figure 3a). The cold layer extends from the bottom—or at least from the deepest instrument, 60 m above the bottom—to about 450-m depth, but for shorter periods it reaches above 400-m depth, covering the entire mooring. The in situ freezing point for a salinity of about S_A=34.75 g/kg is equivalent to $\Theta = -2.25$°C at 460-m depth and $\Theta = -2.30$°C at 525-m depth, so the upper part of the cold layer emerging from the cavity was in situ supercooled. Frazil ice formation at depths between about 400- and 500-m depth was evident in CTD casts on mooring recovery, and accumulation of ice crystals caused instruments to slide up the mooring line

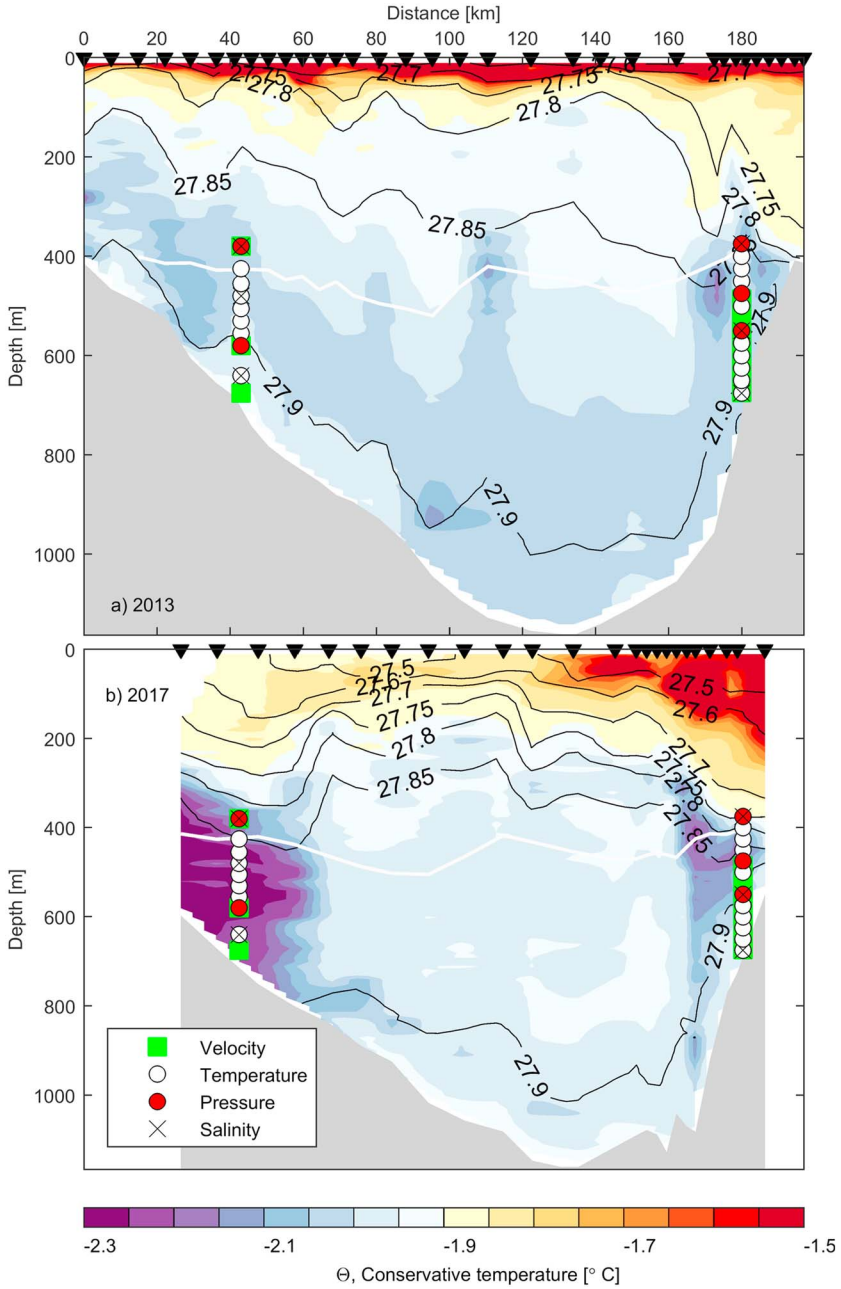

Figure 2. Θ (color) and density (labeled contours) sections from (a) mooring deployment 5–6 January 2013 and (b) the recovery of $M78_{7W}$, 25–28 February 2017. The positions of the casts are indicated by black triangles at the upper axis, the bottom topography is shown in gray, and the estimated ice shelf drafts (see section 2) with a dashed, black line. The position of the sensors on the mooring line is indicated following the legend.

(see section 2). When the cold water is absent (between June and February) the temperatures typically range between $\Theta = -1.9$ and $\Theta = -2.0$°C with shorter episodes of lower temperatures. The seasonal variation in temperature coincides with a seasonal variability of currents (Figure 3c): at depth (675 and 580 m), low temperatures are associated with northward flow while the current is directed eastward during the warmer periods. Low-passed, mean currents are typically around 0.03 m/s in both directions.

The 1 year long temperature records from $M78_{7E}$ on the eastern flank do not show a similar cold pulse. Instead, we observe a *warm* pulse between 400- and 500-m depth in March–May 2013, marking the arrival of the warm inflow (red arrow in Figure 1) to the FIS front (Darelius et al., 2016). Only during a short period in March 2013 do temperatures drop to a minimum of $\Theta = -2.2$°C when a 0.2°C temperature front is advected back and forth

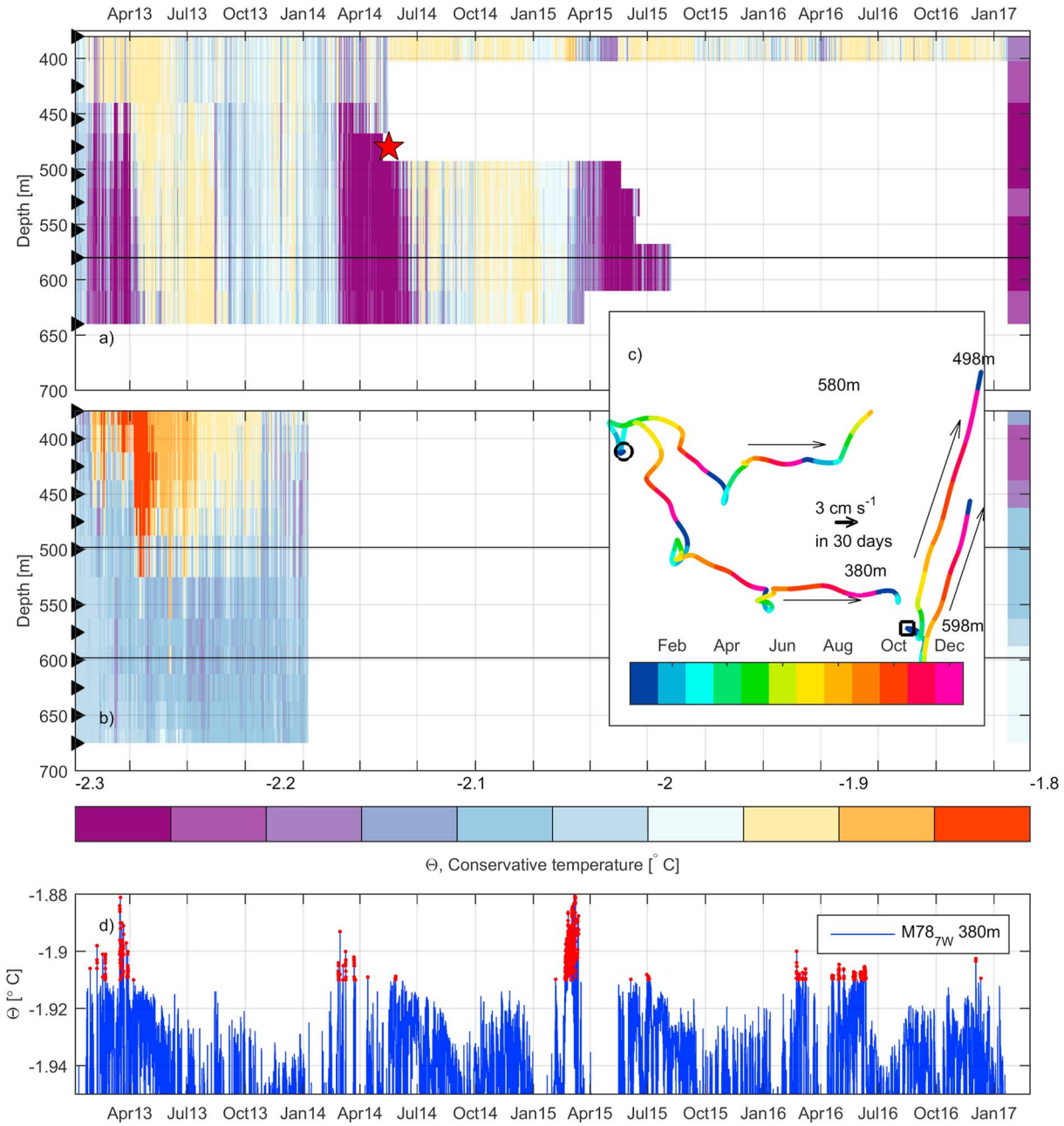

Figure 3. Hovmöller diagram of Θ observed at (a) $M78_{7W}$ and (b) $M78_{7E}$. The temperature profiles obtained after mooring recovery are included. The instrument depths (triangles on the left axis), the depth of the velocity records (lines) in Figure 3c, and the time when instruments slid up the line (red star, see section 2) are indicated. (c) Progressive vector diagram showing currents from $M78_{7W}$ (circle) and $M78_{7E}$ (square) at selected depths (marked by horizontal, black lines in Figures 3b and 3c). The color coding to show the month of the year starting in January 2013. The thick, black arrow to the right shows the distance covered during 1 month if the mean velocity is 0.03 m/s, and the thin, black arrows indicate the direction of flow. Note that the records are of different length. (d) Θ record from $M78_{7W}$, 380 m depth. The scale has been cut in order to highlight periods with higher temperatures, and temperatures above −1.91°C are marked in red.

past the mooring by strong (*O*[0.15 m/s]) tidal currents (not shown). The rest of the time, the temperatures at depth range between Θ = −2.0 and Θ = −2.15°C. The temperatures above the eastern flank are hence higher than those observed in the west during the period of cold outflow but lower than those observed in the west when there is no cold outflow. The currents at $M78_{7E}$ at 500-m depth are directed northward most of the year, and the outflow velocity is increasing throughout the record to reach 10 cm/s in December 2013 (Figure 3c).

The CTD sections obtained along the ice shelf front in 2013 and 2017 (Figure 2) give further insight into the flow across the FIS front. The 2013 section was obtained in early January (Darelius, Makinson et al., 2014),

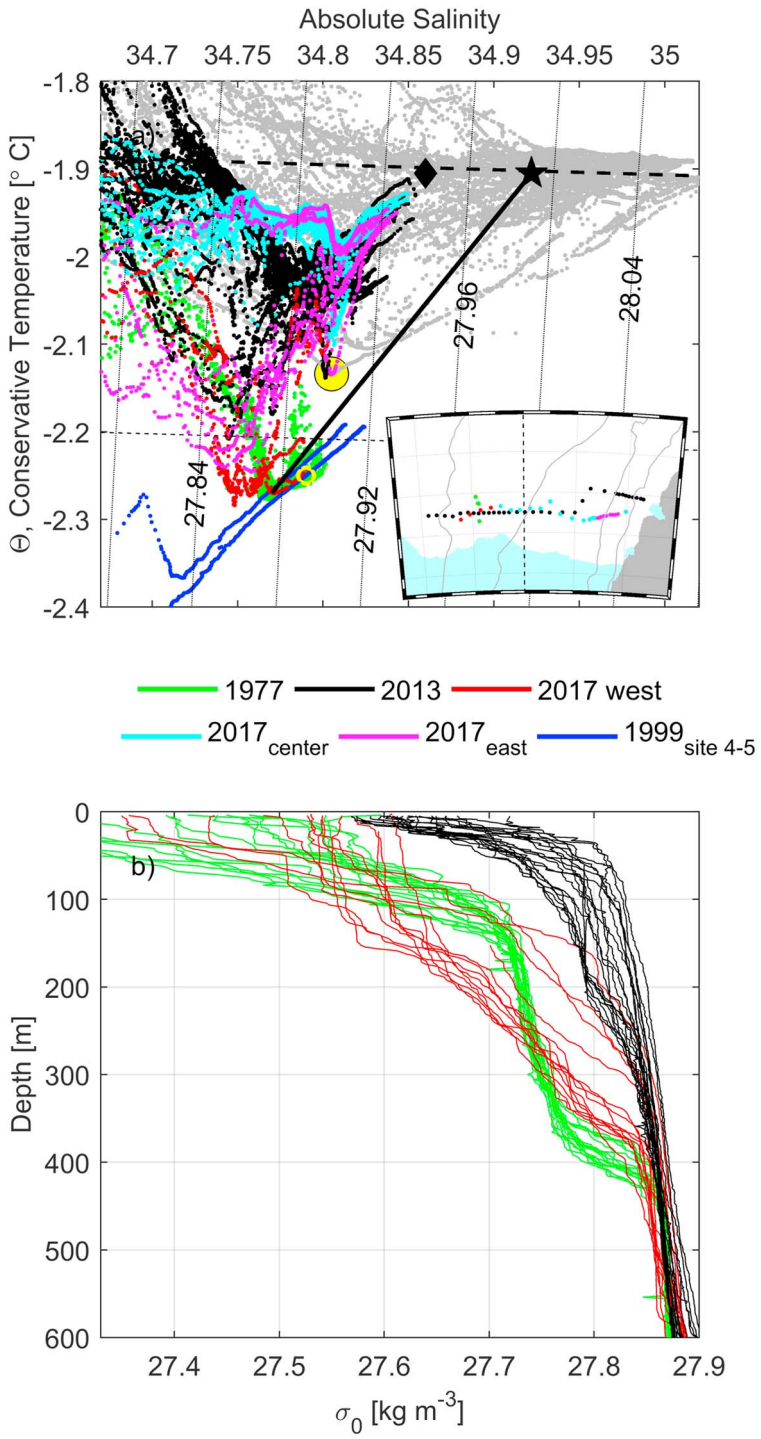

Figure 4. (a) ΘS_A diagram including data from moorings and conductivity-temperature-depth profiles from the ice shelf front (green, February 1977; black, January 2013; and red, cyan, and magenta, February 2017) and the ice shelf cavity (blue, Sites 4 and 5 in 1999, Nicholls et al., 2001 see Figure 1 for location). The dashed lines show the freezing point at the surface (thick, dashed line) and at 400-m depth (thin, dashed line), while the labeled, thin lines show isopycnals referenced to surface pressure. The solid line is a Gade line and the black star marks the inferred source salinity (S_A=34.92 g/kg). The black diamond indicates the source salinity (34.85 g/kg) of the ice shelf water (ISW) observed at the front, for example, in 2013, the yellow, filled circle the interleaving core of colder ISW in the east in 2017, and the small, yellow circle the properties of the cold ISW core observed in 1973 and 1980. The inset shows the position of the ice shelf front profiles. Note that the position of the ice shelf front (Fretwell et al., 2013) is not up to date. (b) Density profiles from the stations shown in Figure 4a and west of 40° (dashed line in inset). The legend is valid for both panels and for the inset.

that is, prior to the seasonal outflow which is observed at $M78_{7W}$ in late January that year. The section only shows traces of the coldest ISW at a few stations above the flanks of the FT (Figures 2a and 4a). The section from 2017, on the other hand, was occupied in late February, a few weeks after the arrival of the seasonal cold pulse. Here the cold water is seen to occupy the region below 400-m depth and west of the 800-m isobath above the western flank of the FT, that is, a region that is at least 30-km wide (Figure 2b). A rough transport estimate obtained by combining the mean velocity from the mooring (0.03 m/s) with the area displaying the cold water in Figure 2b gives 0.3 Sv of northward flow. The CTD sections indicate that the observed seasonality in the outflow at $M78_{7W}$ is not caused by the meandering of a narrow, year-round outflow, but that the outflow is seasonal and spans a wide region over the western flank. A slightly warmer core of cold ISW is observed above the eastern flank of the FT between the 600-m and 1,000-m isobath in the 2017 section.

The $\Theta - S_A$ properties of the ISW emerging at the western mooring from below about 400-m depth indicate the presence of ISW_{Ronne}: the intersection of the Gade line (Gade, 1979) and the surface freezing point line indicates source water with S_A above 34.92, see Figure 4. In $\Theta - S_A$ space, the outflowing ISW overlaps or falls very close ($\Delta\Theta < 0.02$ for a given S_A) to the ISW_{Ronne} observed south of Berkner Island (Site 4 and the deeper part of Site 5, see Figure 1 for location) when the sub-ice shelf water column there was profiled through drilled access holes in 1999 (Nicholls et al., 2001). The inferred source salinity for the coldest ISW in the east is lower than in the west, but its $\Theta - S_A$ properties (Figure 4a) suggest that it may be ISW_{Ronne} diluted by mixing. This is true both in 2013 and 2017, although temperatures are lower in 2017. Below the temperature minimum, within a layer of $ISW_{Berkner}$, there are indications of interleaving of ISW with a higher source salinity, potentially ISW_{Ronne} (Figure 4a, for example, at S_A ~34.82 g/kg, magenta dots within yellow circle).

4. Origin of the Seasonality

To gain insight into the processes that govern the exchange of water masses across an ice shelf front, it is of interest to understand what mechanism causes the seasonal outflow of ISW across the western part of the FIS. Observations and modeling suggest that the seasonality is small within the Filchner cavity (Jenkins et al., 2004; Nicholls et al., 2003) and the seasonal outflow at the FIS front is therefore likely controlled by processes occurring outside of the cavity. What factors may change, allowing the ISW to cross the western part FIS front during summer and autumn but not during the rest of the year? Is the outflow linked to seasonal change in the atmospheric forcing? Or is it changes in the local circulation and the hydrography that lead to the seasonal outflow?

An examination of the local wind field (ERA-interim; Dee et al., 2011) shows no systematic change in wind direction or strength in February that could explain the onset of the seasonal outflow, but low-passed time series reveal that the wind component parallel to the ice shelf front generally is weaker (i.e., less negative) during summer (Figure S1 in the supporting information). The summer winds would hence be less downwelling favorable than the stronger winter winds, although this could be compensated by a less compact sea ice cover resulting in a higher drag coefficient (see, e.g., Andreas et al., 2010). It is not obvious though, how this would directly relate to the observed outflow.

A comparison of the density profiles obtained at the western side of the FIS front during periods with (1977 and 2017) and without (2013) cold outflow (Figure 4b) shows that the stratification is strikingly different. Profiles obtained during cold outflow typically show a density gradient around 400-m depth, that is, roughly at the depth of the ice shelf base (Lambrecht et al., 2007). The nonoutflow profiles, on the other hand, show a density gradient only toward the surface with a thicker, relatively homogeneous layer (Figure 4b) of ISW beneath it (Figure 2a). Note that the density gradient at depth is not created by the outflowing ISW_{Ronne} that has a density similar to that of the ambient ISW. The density gradient is instead caused by the presence of a lighter and slightly warmer water mass above about 400-m depth, that is, above the ISW. The reappearance of this slightly warmer layer at shallower depths during outflow periods in the mooring records is supported by the increase in temperature at the shallowest instrument at the onset of the outflow, for example, in February 2015 (Figure 3d). A similar signal in the stratification is observed above the eastern flank in hydrographic profiles collected by Weddell Seals in 2011 (Årthun et al., 2013).

The circulation at the FIS front was suggested by Darelius, Makinson, et al., (2014) to be determined by potential vorticity (PV) dynamics: the FIS front represents a large step in water column thickness and it thus poses a PV barrier that causes the ISW arriving at the FIS front along eastern coast of Berkner Island to turn eastward

and flow parallel to the ice shelf front to ultimately exit the cavity on the eastern side of the front. A possible explanation for the observed seasonality, which is qualitatively consistent with the available data, is that the presence of a density gradient at or around the level of the ice shelf base decouples the lower part of the water column, effectively weakening the PV barrier and allowing for flow across the FIS front. Similarly, a decoupling by summer time stratification has been evoked to explain the summer inflow of HSSW across the Ronne Ice Shelf front (Nicholls et al., 2009).

A quantitative assessment of the role of stratification in weakening the PV barrier and its relevance for the observed seasonal outflow of ISW across the western part of the FIS front is beyond the scope of our paper. It is possible that the changes in stratification are caused by a local summer restratification or they may be linked to the changes in circulation observed on the continental shelf east of the FT (Ryan et al., 2017), but the possible mechanism needs to be further investigated.

5. Conclusion

This paper presents unique multiyear mooring records from the region just north of the FIS front. Two moorings, placed at the 700-m isobath on either side of the FT, allow us to describe the outflow of ISW from the FIS cavity. The mooring records, supplemented by CTD sections from mooring deployment and recovery, show that ISW originating from the Ronne Trough crosses the western part of the FIS front as a cold pulse during February–June each year. A comparison of density profiles from periods with and without outflow suggests that the ISW outflow occurs when there is a density gradient at the level of the ice shelf base. We hypothesize that the density gradient breaks the PV barrier that is suggested to otherwise steer the ISW eastward along the FIS front (Darelius, Makinson, et al., 2014). The observations do not allow us to determine to what extent, if any, the blocking in the west affects the net outflow of ISW across the FIS front.

Apart from the two sections obtained in 2013 and 2017, there are only two comparable CTD sections obtained along the FIS front in the historical data: a CTD section from 1973 (Carmack & Foster, 1975, reprinted in color by Darelius, Makinson, et al., 2014) and one from 1980 (Foldvik et al., 1985). The two sections both show a core of colder ISW above the western flank with minimum temperatures of about $\Theta = -2.25^{\circ}$C for an S_A of about 34.78–34.80, that is, with core location and ISW properties that overlap those observed in 2017 (Figure 4a). These profiles also display a density gradient around 400 m depth. The western stations in 1980 were occupied in mid-February and the presence of outflowing ISW here at this time of the year is consistent with the timing of the cold pulse in the mooring records. The 1973 section, however, is from early January, that is, prior to the arrival of the seasonal cold pulse in the recent records. The 1973 section might point to interannual variability or possibly a long-term change in the outflow season.

It is possible that the observed seasonal outflow of ISW is a peculiarity observed only at FIS under the hydrographic conditions currently observed in the FT, and that the findings cannot be generalized to other Antarctic ice shelves where the water properties, forcing, and geometry are different. Our results nevertheless reopen the question as to the importance of the ice shelf front as a barrier to the exchange of water between the ice shelf cavity and the ambient ocean. The existence of such a barrier was put forward by early modeling work (e.g., Grosfeld et al., 1997), but later work has questioned its strength and shown that buoyancy-driven boundary currents ought to be able to pass the ice shelf front freely (Holland & Jenkins, 2001; Stern et al., 2014).

The question also arises as to where the ISW emerging across the western part of the FIS front goes. Is there a seasonal, northward flow of ISW along the western flank of the FT, or does the ISW turn eastward at some distance from the FIS front to join the northward current above the eastern FT? The perennial sea-ice cover has so far prevented any observations along the western FT and thus the question remains open.

Acknowledgments
The authors are thankful to H. Bryhni, M. Jensen, K. Vaage, M. Schröder, S. Østerhus, S. Semper, H. LeGoff, A. Laurenzo, V. Tallaindaier, P. Lazeravitchthe, and the crew of RRS Ernest Shackleton (ES060), Polarstern (PS82), and RRS James Clark Ross (JC16004) for assistance with mooring and CTD work. Comments from H. Hellmer (AWI), K. Makinson (BAS), and two anonymous reviewers on earlier versions of the manuscript were greatly appreciated. E. D. received funding from the projects obsFRIS (Polarprog, Norges Forskningsråd) and WARM 23149 (FRINATEK, Norges Forskningsråd). J. B. S. has received funding from the European Research Council (ERC) under the European Union's Horizon 2020 research and innovation program (grant agreement 637770). Mooring data (Darelius & Fer, 2017; Darelius et al., 2018) and CTD data (Darelius & Fer, 2015) can be obtained from www.pangea.de. CTD data from 2017 (Sallée, 2018) can be obtained from www.seanoe.org.

References

Andreas, E. L., Horst, T. W., Grachev, A. A., Persson, P. O. G., Fairall, C. W., Guest, P. S., & Jordan, R. E. (2010). Parametrizing turbulent exchange over summer sea ice and the marginal ice zone. *Quarterly Journal of the Royal Meteorological Society*, *136*(649), 927–943. https://doi.org/10.1002/qj.618

Årthun, M., Makinson, K., Fedak, M. A., & Boehme, L. (2012). Seasonal inflow of warm water onto the southern Weddell Sea continental shelf, Antarctica. *Geophysical Research Letters*, *39*, L17601. https://doi.org/10.1029/2012GL052856

Årthun, M., Nicholls, K. W., & Boehme, L. (2013). Wintertime water mass modification near an Antarctic ice front. *Journal of Physical Oceanography*, *43*(2), 359–365. https://doi.org/10.1175/JPO-D-12-0186.1

Carmack, E. C., & Foster, T. D. (1975). Circulation and distribution of oceanographic properties near the Filchner ice shelf. *Deep Sea Research and Oceanographic Abstracts*, *22*(2), 77–90. https://doi.org/10.1016/0011-7471(75)90097-2

Darelius, E., & Fer, I. (2015). Physical oceanography from CTD in the Filchner Depression (Weddell Sea, Antarctica) during Ernest Shackleton cruise ES060. https://doi.org/10.1594/PANGAEA.846962
Darelius, E., & Fer, I. (2017). Physical oceanography from mooring SB, SC, SD and SE in the Weddell Sea. https://doi.org/10.1594/PANGAEA.870518
Darelius, E., Fer, I., & Nicholls, K. W. (2016). Observed vulnerability of Filchner-Ronne ice shelf to wind-driven inflow of warm deep water. *Nature Communications*, *7*, 12300. https://doi.org/10.1038/ncomms12300
Darelius, E., Fer, I., & Sallée, J. B. (2018). Physical oceanography from mooring SA in the Weddell Sea. https://doi.org/10.1594/PANGAEA.883905
Darelius, E., Makinson, K., Daae, K., Fer, I., Holland, P. R., & Nicholls, K. (2014). Hydrography and circulation in the Filchner Depression, Weddell Sea, Antarctica. *Journal of Geophysical Research: Oceans*, *119*, 5797–5814. https://doi.org/10.1002/2014JC010225
Darelius, E., Smedsrud, L. H., Østerhus, S., Foldvik, A., & Gammelsrød, T. (2009). Structure and variability of the Filchner overflow plume. *Tellus A*, *61*(3), 446–464. https://doi.org/10.1111/j.1600-0870.2009.00391.x
Darelius, E., Strand, K. O., Østerhus, S., Gammelsrød, T., Årthun, M., & Fer, I. (2014). On the seasonal signal of the Filchner overflow, Weddell Sea, Antarctica. *Journal of Physical Oceanography*, *44*, 1230–1243. https://doi.org/10.1175/JPO-D-13-0180.1
Dee, D. P., Uppala, S. M., Simmons, A. J., Berrisford, P., Poli, P., Kobayashi, S., et al. (2011). The ERA-Interim reanalysis: Configuration and performance of the data assimilation system. *Quarterly Journal of the Royal Meteorological Society*, *137*(656), 553–597. https://doi.org/10.1002/qj.828
Fer, I., Makinson, K., & Nicholls, K. W. (2012). Observations of thermohaline convection adjacent to Brunt ice shelf. *Journal of Physical Oceanography*, *42*(3), 502–508. https://doi.org/10.1175/JPO-D-11-0211.1
Foldvik, A., Gammelsrød, T., Østerhus, S., Fahrbach, E., Rohardt, G., Schröder, M., et al. (2004). Ice shelf water overflow and bottom water formation in the southern Weddell Sea. *Journal of Geophysical Research*, *109*, C02015. https://doi.org/10.1029/2003JC002008
Foldvik, A., Gammelsrød, T., & Tørresen, T. (1985). Circulation and water masses on the southern Weddell Sea shelf. In S. S. Jacob (Ed.), *Oceanology of the Antarctic Continental Shelf, Antarctic Research Series 43* (pp. 5–20). Washington DC: American Geophysical Union.
Foldvik, A., & Kvinge, T. (1974). Conditional instability of sea water at the freezing point. *Deep Sea Research and Oceanographic Abstracts*, *21*(3), 169–174.
Fretwell, P., Pritchard, H. D., Vaughan, D. G., Bamber, J. L., Barrand, N. E., Bell, R., et al. (2013). Bedmap2: Improved ice bed, surface and thickness datasets for Antarctica. *The Cryosphere*, *7*(1), 375–393. https://doi.org/10.5194/tc-7-375-2013
Fürst, J. J., Durand, G., Gillet-Chaulet, Tavard, L., Rankl, M., Braun, M., & Gagliardini, O. (2016). The safety band of Antarctic ice shelves. *Nature Climate Change*, *6*(5), 479–482. https://doi.org/10.1038/nclimate2912
Gade, H. (1979). Melting of ice in sea water: A primitive model with application to the Antarctic ice shelf and icebergs. *Journal of Physical Oceanography*, *9*(1), 189–198. https://doi.org/10.1175/1520-0485(1979)009<0189:MOIISW>2.0.CO;2
Grosfeld, K., Gerdes, R., & Determann, J. (1997). Thermohaline circulation and interaction between ice shelf cavities and the adjacent open ocean. *Journal of Geophysical Research*, *102*(C7), 15,595–15,610. https://doi.org/10.1029/97JC00891
Hellmer, H. H. (2004). Impact of Antarctic ice shelf basal melting on sea ice and deep ocean properties. *Geophysical Research Letters*, *31*, L10307. https://doi.org/10.1029/2004GL019506
Hellmer, H. H., Kauker, F., Timmermann, R., Determann, J., & Rae, J. (2012). Twenty-first-century warming of a large Antarctic ice-shelf cavity by a redirected coastal current. *Nature*, *485*(7397), 225–8. https://doi.org/10.1038/nature11064
Hellmer, H. H., Kauker, F., Timmermann, R., Hattermann, T., Shelf, F.-R. I., & Mengel, M. (2017). The fate of the southern Weddell Sea continental shelf in a warming climate. *Journal of Climate*, *30*(12), 4337–4350. https://doi.org/10.1175/JCLI-D-16-0420.1
Holland, D., & Jenkins, A. (2001). Adaptation of an isopycnic coordinate ocean model for the study of circulation beneath ice shelves. *Monthly Weather Review*, *129*(8), 1905–1927. https://doi.org/10.1175/1520-0493(2001)129<1905:AOAICO>2.0.CO;2
IOC, SCOR, & IAPSO (2010). The international thermodynamic equation of seawater - 2010: Calculations and use of thermodynamic properties (196 pp.)
Jenkins, A., Holland, D. M., Nicholls, K. W., Schröder, M., & Østerhus, S. (2004). Seasonal ventilation of the cavity beneath Filchner-Ronne ice shelf simulated with an isopycnic coordinate ocean model. *Journal of Geophysical Research*, *109*, C01024. https://doi.org/10.1029/2001JC001086
Lambrecht, A., Sandhäger, H., Vaughan, D., & Mayer, C. (2007). New ice thickness maps of Filchner-Ronne ice shelf, Antarctica, with specific focus on grounding lines and marine ice. *Antarctic Science*, *19*(04), 521–532. https://doi.org/10.1017/S0954102007000661
McDougall, T. J., Jackett, D. R., Millero, F. J., Pawlowicz, R., & Barker, P. (2012). A global algorithm for estimating absolute salinity. *Ocean Science*, *8*(6), 1123–1134. https://doi.org/10.5194/os-8-1123-2012
Nicholls, K., Østerhus, S., Makinson, K., & Johnson, M. (2001). Oceanographic conditions south of Berkner Island, beneath Filchner-Ronne Ice Shelf, Antarctica. *Journal of Geophysical Research*, *106*(C6), 481–11.
Nicholls, K. W., & Østerhus, S. (2004). Interannual variability and ventilation timescales in the ocean cavity beneath Filchner-Ronne ice shelf, Antarctica. *Journal of Geophysical Research*, *109*, C04014. https://doi.org/10.1029/2003JC002149
Nicholls, K. W., Østerhus, S., Makinson, K., Gammelsrød, T., & Fahrbach, E. (2009). Ice-ocean processes over the continental shelf of the southern Weddell Sea, Antarctica: A review. *Reviews of Geophysics*, *47*, RG3003. https://doi.org/10.1029/2007RG000250
Nicholls, K. W., Padman, L., Schröder, M., Woodgate, R. A., & Jenkins, A. (2003). Water mass modification over the continental shelf north of Ronne ice shelf, Antarctica. *Journal of Geophysical Research*, *108*(C8), 3260. https://doi.org/10.1029/2002JC001713
Pritchard, H. D., Ligtenberg, S. R. M., Fricker, H. A., Vaughan, D. G., Broeke, M. R. V. D., Padman, L., & van den Broeke, M. R. (2012). Antarctic ice-sheet loss driven by basal melting of ice shelves. *Nature*, *484*(7395), 502–505. https://doi.org/10.1038/nature10968
Rignot, E., Jacobs, S., Mouginot, J., & Scheuchl, B. (2013). Ice-shelf melting around Antarctica. *Science*, *341*(6143), 266–70. https://doi.org/10.1126/science.1235798
Ryan, S., Hattermann, T., Darelius, E., & Schröder, M. (2017). Seasonal cycle of hydrography on the eastern shelf of the Filchner Trough, Weddell Sea, Antarctica. *Journal Geophysical Research: Oceans*, *122*, 6437–6453. https://doi.org/10.1002/2017JC012916
Sallée, J. B. (2018). Hydrological and current data for the Southern Weddell Sea, collected as part of the WAPITI oceanographic survey (JR16004). https://doi.org/10.17882/54012
Semper, S., & Darelius, E. (2017). Seasonal resonance of diurnal continental shelf waves in the southern Weddell Sea, Antarctica. *Ocean Science*, *13*, 77–93. https://doi.org/10.5194/os-13-77-2017
Stern, A., Holland, D. M., Holland, P. R., Jenkins, A., & Sommeria, J. (2014). The effect of geometry on ice shelf ocean cavity ventilation: A laboratory experiment. *Experiments in Fluids*, *55*(5), 1719. https://doi.org/10.1007/s00348-014-1719-3